Pyridinophane cryptand hosts with dicopper(I) or dicopper(II) preferences

Debbie J. Marrs[a,b], Vickie McKee[b,*], Jane Nelson[a,b,*], Qin Lu[a,b] and Charles J. Harding[a]
[a]*Open University, 40 University Road, Belfast BT7 1SU (UK)*
[b]*Chemistry Department, Queens University, Belfast BT9 5AG (UK)*

(Received April 14, 1993)

Abstract

A hexaimino pyridinophane cryptand, L^4, derived by [2+3] Schiff base condensation of tris-2-ethylamino amine (tren) with diformylpyridine fails to host Cu(II) but accommodates dicopper(I) with reasonable oxidative stability; the octaamino derivative, L^5, functions as a good host for dicopper(II). A single crystal X-ray structure determination was carried out on $[Cu_2L^4](ClO_4)_2CH_2Cl_2$, monoclinic, unit cell dimensions, $a = 27.256(8)$, $b = 10.970(3)$, $c = 18.941(6)$ Å, $\beta = 128.37(3)°$, $U = 4440(2)$ Å^3. Each Cu(I) ion is coordinated to three imino donors and shows weaker interactions with other donors. The Cu(I)–Cu(I) distance is 3.038 Å.

The importance of sp^2N donors in bioinorganic copper chemistry [1] is reinforced with each new copper protein crystal structure. As the metal coordination site in the protein is usually associated with steric protection, the potential of our new azacryptand ligands [2] to encapsulate copper cations is of special interest in this connection. We have already described the structure of three dicopper cryptates of the azacryptand series. L^1 and its octaamino derivative L^2 act as hosts for pairs of Cu(I) or Cu(II) ions [3, 4]. The relatively long 1,6 spacer in these ligands leads to internuclear separations of ≈6 Å. In contrast, a dicopper(I) complex of the smallest cryptand (L^3) shows an exceptionally short Cu–Cu distance of 2.45 Å which is enforced by ligand dimensions [5]. Markedly different interactions between copper ions would be expected to result from these very different internuclear separations. This expectation is confirmed by the results of magnetic, ESR [3, 4] and electrochemical [6] measurements. For the longer separation, virtually no evidence of interaction in the absence of bridging ligand is seen, while across the 2.45 Å internuclear distance almost complete electron delocalization operates [5] between the copper ions leading to its description as an average-valence $Cu^{1.5}$ ---$Cu^{1.5}$ system. In aiming for a sequential two-electron redox system of potential catalytic value, we require an internuclear separation intermediate between these extremes, i.e. large enough to accommodate at least a single-atom bridging donor while short enough to ensure good communication between the copper centres. This led to selection of the cryptands L^4 and L^5.

L^4 can be easily made on a Group II template; however, we have found it almost impossible to remove the Gp II cation after template synthesis [7], so the ligand was prepared metal-free by [2+3] condensation of tris-2-ethylaminoamine (tren) with diformylpyridine (in 50–60% yield). The reduced ligand L^5 can be generated, by *in situ* borohydride reduction, from the L^4 solution. Treatment of these ligands with Cu(I) and Cu(II) cations led to very different behaviour; L^4 showing preference for Cu^+ and L^5 for Cu^{2+}.

Hexaimine ligand, L^4

Treatment of this ligand with copper(II) gave disappointing results. In the absence of base, only crude samples of colourless, apparently protonated species could be obtained; where base was added, the resultant impure green powders showed ν(CO) IR absorption, suggesting ring opening.

However, on treatment of L^4 with Cu(I), followed by rapid reduction of volume, a dark brown crystalline product, $[Cu_2L^4[X]_2$ (**1** or **2**) (Tables 1 and 2), was easily obtained. The template strategy was unsuccessful; in contrast to the situation with other cryptands of the series [6], pure products could not be obtained from reaction of dicarbonyl with triamine in the presence of copper(I) salts. This is perhaps because, as ^1H NMR spectra demonstrate, the dicopper(I) cryptates undergo

*Authors to whom correspondence should be addressed.

0020-1693/93/$6.00

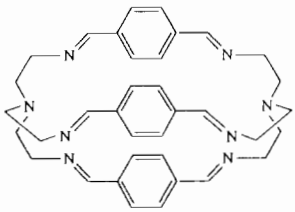

L^1

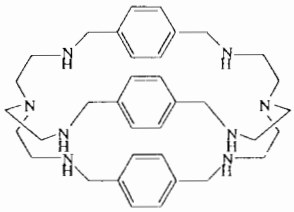

L^2

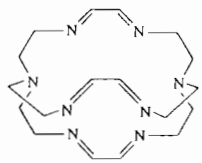

L^3

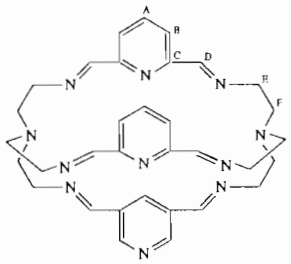

L^4

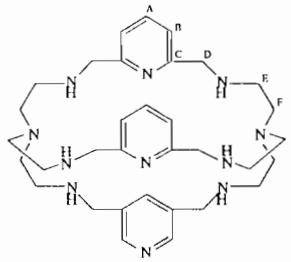

L^5

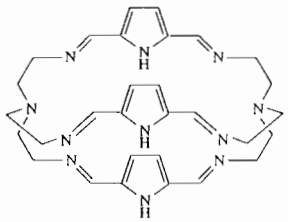

L^6

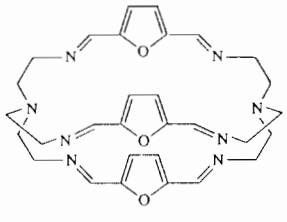

L^7

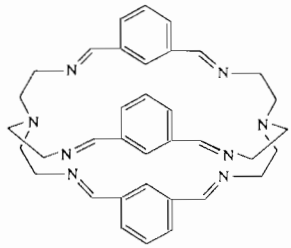

L^8

TABLE 1. ^1H NMR spectra[a] of L^4, L^5 and derivatives

Compound	ν	T	H_A	H_B	H_D	H_E	H_F	Reference
L^4[b]	400	294	8.11d	7.81tr	7.59s	3.57br, s	2.87s	7, 12
	500	223	8.08d	7.84tr	7.50s	3.78d; 3.25tr	2.88tr, 2.78d	7, 12
$[CaL^4](ClO_4)_2 \cdot 2H_2O$[c]	300	294	7.80d	8.25tr	8.41s	3.05m	2.80d; 2.48tr	7
$[SrL^4](ClO_4)_2$[c]	300	294	7.80d	8.27tr	8.50s	3.20tr (3.14d, 2.48d)	2.40tr	7, 12
$[BaL^4](ClO_4)_2$[c]	250	294	7.80d	8.23tr	8.53s	3.45tr (3.0m)	2.48tr	7, 12
$[Cu_2L^4](ClO_4)_2 \cdot 2CH_2Cl_2$[c]	400	294	7.80d	8.14br, tr	8.52s	*c.* 3.2br	3.0br, d; 2.6br, tr	this work
	500	233	7.89d	8.18tr	8.52s	3.21d; 3.08tr; 3.16d	2.67tr	
L^5[b]	300	294	7.05d	7.47tr	3.86s	2.62q (2.65 NH)		this work

[a]Shifts in ppm from TMS. [b]$CDCl_3$ solution. [c]CD_3CN solution.

reaction in solution. ^1H NMR (233 K) spectra of **2** followed over time showed growth of features around 8.55(s), 8.0(m), 3.5(d) as well as absorption overlapped with methylene signals in the 2.6–3.2 ppm region. This overlapping hinders assignment of the individual signals in the axial/equatorial methylene pattern, although it is clear (in the frozen-out conformation which is apparent at low temperatures) that as in other dicopper(I) cryptates [7, 8], a triplet due to the axial methylene proton adjacent to the bridgehead ($H_{F(ax)}$) lies clear of the other signals at highest field. NOE enhancement of the doublet at ≈3.2 ppm upon irradiation of the imine signal shows that $H_{E(eq)}$ is the lowest field component of the methylene signal. $H_{F(eq)}$ and $H_{E(ax)}$ comprise an overlapping pair of signals complicated by the appearance of impurity bands; however in the −20 °C 500 MHz spectrum the impurity bands are severely broadened, which removes their interference. The doublet signal $H_{F(eq)}$ can then be clearly seen at 3.16 and the triplet $H_{E(ax)}$ at 3.08 ppm. The pattern is not unlike that seen (Table 1) for Ca^{2+} and Sr^{2+} cryptates [7] of L^4, where $H_{F(ax)}$, $H_{F(eq)}$ and $H_{E(ax)}$ lie at closely

TABLE 2. Analytical, selected spectroscopic and magnetic susceptibility data for L^4 and L^5 complexes

Compound	No.	Colour	Analytical data (%)			Selected IR data (cm^{-1})		dd Bands[c]/k (Σ)	μ (BM)[d]	
			N	C	H	ν(NH)/ ν(C=N)	νClO_4 or BF_4		300 K	90 K
L^4		white	25.9(26.1)	67.4(67.2)	6.6(6.6)	1647				
$L^5 \cdot 4H_2O$		white	22.4(22.9)	58.2(58.8)	8.8(8.8)	3275				
$[Cu_2L^4](BF_4)_2$	**1**	dark brown	16.9(17.3)	44.7(44.5)	4.3(4.4)	1641	1072s 1060s			
$[Cu_2L^4](ClO_4)_2 \cdot CH_2Cl_2$	**2**	dark brown	14.2(14.2)	38.7(38.7)	3.6(3.9)	1634	1119s; 635ms 1105s; 621ms 1087vs			
$[Cu_2L^4](BF_4)_3 \cdot 4H_2O$	**3**	mid brown	14.3(14.8)	37.8(38.1)	4.4(4.5)	1653	1080s 1057s	13600(80) 16700(100)	2.2	1.9
$[Cu_2L^5)(ClO_4)_4 \cdot MeCN$	**4**	bright blue	14.0(14.3)	35.8(35.8)	4.3(4.6)	3259	1118sh; 623ms 1099vs	12300(440) 15400(330)	1.9	1.8
$[Cu_2L^5](ClO_4)_4 \cdot 4H_2O$	**5**	bright blue	12.7(12.8)	33.0(33.0)	4.4(4.9)	3259	1141vs; 635ms 1118vs; 625ms 1087vs	[b]	[b]	
$[Cu_2L^5N_3](ClO_4)_3 \cdot 3H_2O$	**6**	bright green	17.2(17.5)	35.1(35.3)	4.8(5.1)	3285	1110s; 624ms 2045s[a]	11900(550) 14400(470)	1.9	1.8

[a] νN_3^-. [b] Not investigated. [c] MeCN solution. [d] Per Cu(II) ion. Calculated values in parentheses.

similar chemical shift, indicating similar conformations for the ligand in the convergent donor situation induced by the presence of one or more guest cations. However, it is unusual for $H_{E(ax)}$ to lie at higher field than either $H_{E(eq)}$ or $H_{F(eq)}$. This suggests a conformation which brings $H_{F(eq)}$ under the influence of the deshielding cone of the aromatic circulation associated with the pyridine rings.

Although the crystal structure obtained for **2** (q.v.) indicates some lack of symmetry in the solid state, the slight difference in siting of, for example, imine protons does not appear to be sufficient to split the signal. This is unlike the spectrum presented by the highly unsymmetric complex [9] $[Cu_2L^6]X_2$, where both imine and aromatic signals appear as three clearly resolved absorptions due to chemical shift differences arising from their inequivalent siting.

As with almost all the disilver(I) [8], but not dicopper(I) cryptates we have studied, fluxionality was evident in the ^1H NMR spectrum of **2**. At ambient temperature, broad signals are observed for the methylene CH_2 protons, but by 233 K the axial methylene protons present as triplets and equatorial protons as doublets, as observed in other systems of this kind [10, 11]. This is similar to the behaviour of the free ligand, L^4, which is mobile [12] at ambient but frozen out into doublet and triplet components by 213 K (Table 1). The coalescence temperature, T_c, for H_E at 500 MHz is similar (at 293 and 298 °C, respectively) for L^4 (in $CDCl_3$) and for **2** (in CD_3CN).

Nonetheless, on account of the greater separation of the frozen-out signals in L^4, this indicates significantly higher ΔG^* for methylene protons in this ligand in its complexed form, **2**, as expected. In comparison with the free ligand, where positive NOE is experienced [12], irradiation into the imino-proton signal of **2** shows normal negative NOE enhancement of the aromatic doublet and of $H_{E(eq)}$ implying (as expected for a convergent conformation) that the imino-N is directed into the cavity, and the imino-CH outwards making a close approach to the aromatic α-protons and to $H_{E(eq)}$.

An X-ray diffraction crystallographic structure determination confirms this and illustrates the encapsulation of copper(I) within the cryptand.

X-ray crystallographic structure determination of 2

The $[Cu_2L^4]^{2+}$ cation (Fig. 1 and Table 3) lies on a crystallographic two-fold axis which passes through N(6) and C(17) bisecting the Cu–Cu vector. Two symmetry-related copper ions are bound within the cavity, each coordinated to three imine nitrogen donors with Cu–N(imine) distances of ≈ 2.02 Å. The copper atoms are displaced by 0.63 Å from the mean plane of the three imine nitrogen atoms towards the centre of the cavity. There are weaker interactions with the bridgehead amine (Cu–N(1) = 2.753(4) Å), one of the pyridine nitrogen donors (Cu–N(3) = 2.640(4) Å and the second copper atom (Cu–Cu′ = 3.038(2) Å). In addition, there may be some interaction with the remaining pyridine

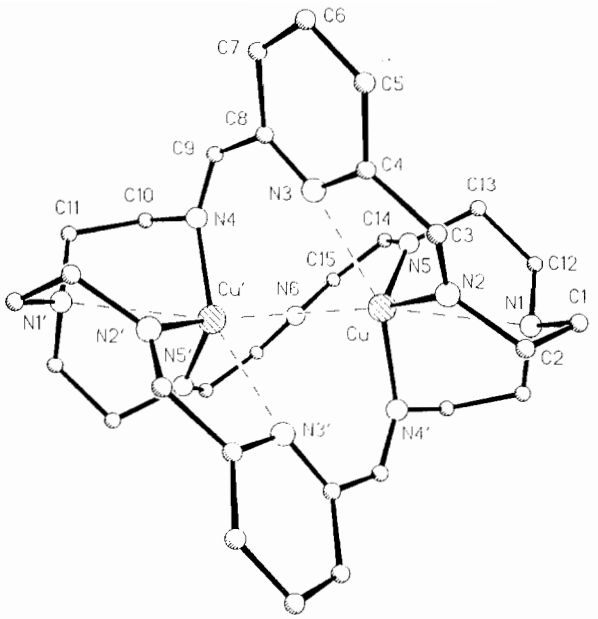

Fig. 1. Perspective view of the $[Cu_2L^4]$ cation. For distances, see Table 3.

TABLE 3. Selected interatomic distances (Å) and angles (°)

Cu–N(1)	2.753(4)	Cu–N(2)	2.028(4)
Cu–N(3)	2.640(4)	Cu–N(5)	2.011(4)
Cu–Cu′	3.038(2)	Cu–N(4′)	2.019(3)
N(2)–Cu–N(3)	71.2(2)	N(2)–Cu–N(5)	115.9(2)
N(3)–Cu–N(5)	92.6(1)	N(2)–Cu–N(4′)	106.8(2)
N(3)–Cu–N(4′)	155.2(2)	N(5)–Cu–N(4′)	109.6(2)
N(1)–Cu–Cu′	168.3(2)	N(2)–Cu–Cu′	114.5(2)
N(3)–Cu–Cu′	64.8(1)	N(4′)–Cu–Cu′	95.7(2)
N(5)–Cu–Cu′	112.2(2)		

nitrogen atoms (Cu–N(3′) = 3.061(5), Cu–N(6) = 3.014(5) Å.) Atoms N(1), Cu, Cu′ and N(1′) are not colinear, the copper atoms being displaced from the N(1)–N(1′) line towards N(3) and N(3′) (N(1)–Cu–Cu′ = 168.3(2)°). Neither the perchlorate anions nor the dichloromethane solvate molecules show any interaction with the cation.

In so far as the Cu(I) ions may be considered as three-coordinate, this is the first example of such coordination geometry in our cryptand series. Failure to strongly coordinate either bridgehead or pyridine-N may derive from steric constraints. The various conformations available to the ligand in its free and coordinated state are presently under study using molecular modelling techniques [12] which may reveal the presence of strain in the binuclear cryptate. There is indeed, as we will see, chemical evidence for hydrolytic instability in solution, which supports this suggestion.

Redox behaviour

Cyclic voltammetry of **1** shows [6] a pair of overlapped quasi-reversible waves, with oxidation components at −110 and +12 mV versus Fc^+/Fc. Despite the absence of any obvious air sensitivity, it thus appears, on thermodynamic grounds, that molecular oxygen should be capable of oxidizing the copper(I) ions. In order to monitor any degree of oxidation unassociated with a noticeable colour change, a dmf solution was left open to atmosphere in an ESR cell for several days and the ESR signal monitored over that period.

In the course of around a week, a broad 4-line signal ($g_\parallel \approx 2.14$, $A_\parallel \approx 160$ G, $g_\perp \approx 2.00$) grew slowly. (The lack of definition of this ESR signal is to be expected, given that ^1H NMR spectra demonstrate significant decomposition of the dicopper(I) complex in solution within this time scale.) In contrast, the response to treatment with Fc^+ is immediate; an immediate lowering of intensity of the dark brown colour (corresponding to loss of the intense (Σ 5000) ≈ 450 nm MLCT absorption) was noticed, accompanied by the development of an ESR signal. (Oxidation could be carried out with Ag^+ but ESR of the Ag^+-oxidized solution indicated the presence of solvated Cu^{2+} species, suggesting 'scrambling' of cations, so Fc^+ was normally used.) The ESR signal of the freshly oxidized solution was broad, initially containing an 'axial' 4-line ($g_\parallel = 2.33$, $A_\parallel \approx 120$ G, $g_\perp = 2.05$) hyperfine pattern which is gradually replaced (after a day in dmf or several days in MeCN) by a different 4-line spectrum with $A_\parallel \approx 160$ G and other parameters resembling the spectrum of the product obtained by air oxidation. This second ESR spectrum was associated with development of a red–bronze colour resulting from growth of a 480 nm absorption in the electronic spectrum. Solids recovered from such aged solutions show ν(CO) and ν(NH) absorptions in the IR, suggesting that the ligand has been modified by hydrolysis. Observation of the same ESR pattern from the (slowly) air-oxidized as from aged Fc^+-oxidized solutions suggests that the end product does not depend on whether oxidation precedes hydrolysis.

In an attempt to isolate the mixed-valence product before any decomposition had set in, a 1:1 mixture of **1** with $FcBF_4$ in MeCN solution was rapidly reduced to dryness and washed well with $CHCl_3$ to remove ferrocene. The mid-brown product **3** had magnetic susceptibility corresponding (Table 2) to one unpaired spin. The ESR spectrum of this product, even in freshly made solution, showed evidence of the 160 G hyperfine pattern as a minor constituent together with the expected $A_\parallel = 120$ G signal. Aged solutions had converted entirely to the $A_\parallel = 160$ G product.

Oxidation attempts using 2:1 stoichiometry did not generate any new ESR pattern, though use of excess

Ag^+ was associated with the appearance of the 'free' Cu^{2+} ESR spectrum, and indeed on some occasions, isolation of a silver complex of L^4 [12].

It appears, then, that copper(II) is not favoured as a guest within this cryptand, and even dicopper(I) is not long-term stable. The one-electron oxidized mixed-valence form of the cryptate exists, but may have too transient an existence in solution to be of value for practical purposes, e.g. in catalysis. However, because **2** meets many of the criteria [13, 14] for copper biosite models in respect of, for example, Cu---Cu separation, redox potential and coordinative unsaturation, we believe that at least preliminary investigation of redox catalytic function may be worthwhile, and this is planned.

As in many other systems of this kind, instability of the imino-cryptand focussed attention on the octaamino derivative L^5 which, with all six imine functions hydrogenated, offers stability advantages in respect of hydrolysis.

Octaamine ligand, L^5

The oxidation state preferences of copper within the amine and imine hosts are markedly different. As we have mentioned, the dicopper(I) L^4 cryptates, **1** and **2** are readily obtained, but the analogous complex of copper(I) within L^5 is so easily oxidized that we have failed to obtain Cu(I) salts of acceptable purity. On the other hand, dicopper(II) L^5 cryptates are readily obtained. Alone of the dicopper(II) cryptates prepared so far [15], these fail to crystallize as μ-OH dimers, even in the presence of deliberately added base. Instead we obtain the bright blue tetracationic salt, $Cu_2L^5(ClO_4)_4$ as the hydrate **5**, or following recrystallization, as the MeCN solvate **4**. (Physical measurements were carried out on the more crystalline product, **4**.)

ESR spectroscopic and magnetic susceptibility measurements on **4** alike testify to the presence of weakish interaction between the Cu(II) paramagnets (Table 2). The dmf glass spectrum (Fig. 2) shows a nicely resolved ($A_{iso} = 60$ G) 7-line half-band at $\approx 1/500$th intensity of the $g = 2$ signal, while this main band signal, although broad but lacking any resolved zero-field splitting, shows signs of poorly resolved hyperfine coupling with $A_{\|}$ around 70–80 G, a value characteristic of the interacting dicopper assembly. In addition, the magnetic moment of the tetraperchlorate salt reduces somewhat with temperature over the range 80–300 K, consistent with a magnetic exchange coupling constant, $-2J$, of the order of 20 cm^{-1} (see 'Supplementary material').

In contrast to results obtained on **1**, electrochemistry indicates that the copper centres in **4** undergo redox more or less independently of each other; just a single (fairly broad) two-electron quasi-reversible wave is seen

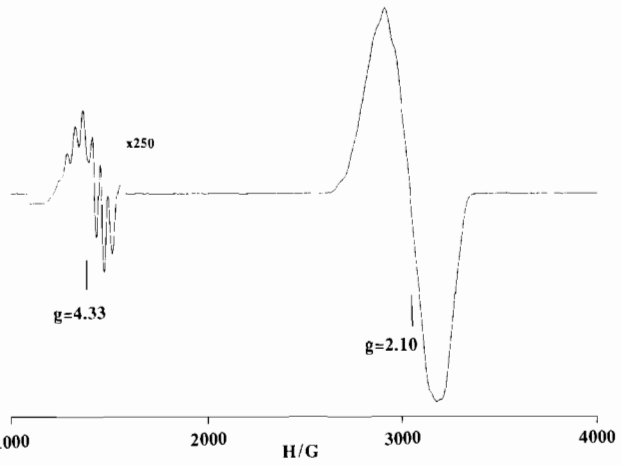

Fig. 2. X-band ESR spectrum of **4** (dmf glass) at 100 K.

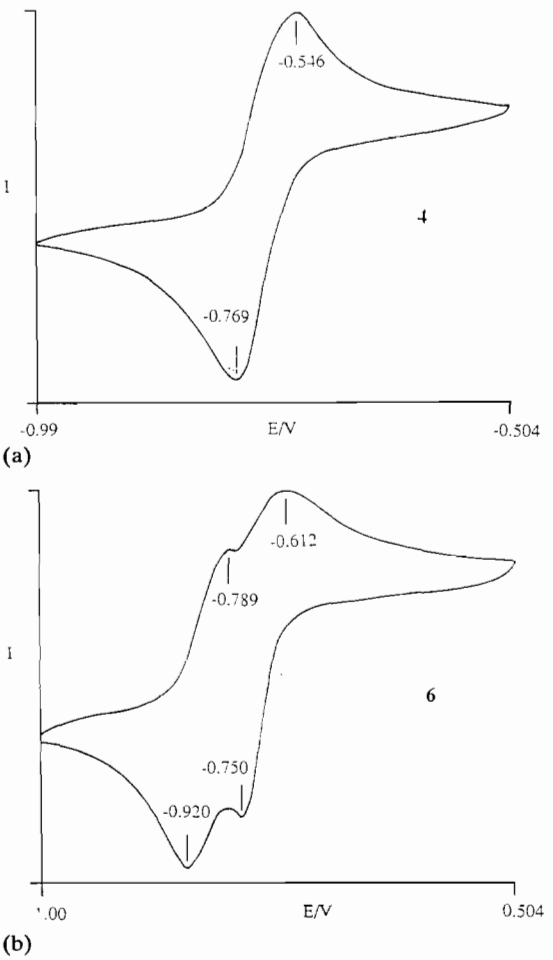

Fig. 3. Cyclic voltammetry of **4** (a) and **6** (b), quoted vs. ferrocene, scan rate 50 mV s^{-1}.

(Fig. 3(a)) at ≈ -650 mV versus Fc/Fc^+, the relatively negative reduction potential testifying to the increased thermodynamic stability of the +2 state of copper cryptated within the saturated azacryptand. Neither

magnetic nor electrochemical properties suggest a particularly efficient mode of communication between the copper centres in **4**, in comparison with the virtually diamagnetic [15] μ-hydroxo dicopper(II) complexes of hexaiminocryptands, L^7 or L^8, for example. Presumably this derives largely from the absence of a bridging ligand, which limits interaction to the 'through-space' dipole–dipole mechanism [16].

We attempted incorporation of a bridging ligand, but treatment with imidazolate and pyrazolate failed to generate any altered product; however, with azide in appropriate stoichiometry we obtained a green microcrystalline product, $[Cu_2(N_3)][ClO_4]_3 \cdot 3H_2O$ (**6**). This product showed intense IR absorption at 2045 cm^{-1} together with a medium weak 1290 cm^{-1} peak both of which can be attributed to coordinated azide. The appearance of ν_s with appreciable intensity indicates a low symmetry site for azide, either terminal, 1,1-bridged or bent 1,3-bridged. There is no indication of the unusual spectroscopic properties which mark the linear 1,3-bridged assembly seen in other azido-bridged cryptates of this series [4]. For example, the ESR spectrum fails to show the large zero-field effects which were observed in the linearly bridged system, merely a 150 G splitting of the $g=2$ signal, which is easily explained on the dipolar mechanism [16], given a Cu–Cu separation of $\approx$4–5 Å. The absence of clearly defined triplet features in the ESR spectrum may be taken to suggest a bent 1,3 bridging mode although the possibility of terminally coordinated azide cannot be ruled out. (Study of isotopic shifts in the vibrational spectrum of the ^{15}N enriched azide complex, which are planned, should throw more light on this problem [17].)

Little magnetic interaction operates between the Cu(II) paramagnets, the temperature dependence of susceptibility corresponding to a magnetic exchange coupling constant*, $-2J$, of only 2 cm^{-1}. This is lower than the antiferromagnetic coupling constant observed for **4** and represents a low value even for unsymmetrically bridged azide [18], so it seems clear that if a bridge exists, it is long and weak. The absence of any $Cu_2N_3L^5$ or CuN_3L^5 peaks in the FAB-mass spectrum (in contrast to the linearly bridged complexes, where such peaks are dominant [4]) is further evidence for weak coordination of the azido ligand.

However, the presence of azide has an effect on the electrochemistry. A pair of quasi-reversible waves (Fig. 3(b)) centred around -680 and -855 mV versus Fc/Fc^+ now replace the single two-electron wave seen for the unbridged dicopper(II) complex. The azide link assists electronic communication between the copper centres so that the assembly now undergoes redox in two sequential steps: ($X=N_3^-$)

$$[Cu(I)Cu(I)XL^5] \longleftrightarrow [Cu(I)Cu(II)XL^5] \longleftrightarrow [Cu(II)Cu(II)XL^5] \quad (1)$$

*See 'Supplementary material'.

Conclusions

The present investigations have revealed that the dicopper(I) complex of the hexaimine cryptand has suitable redox potential and coordination geometry for redox catalysis, but poor hydrolytic stability which may limit its application. There also exists the promise that the more robust dicopper(II) complex of the octaamine derivative, whose redox potentials are less ideal, may still be of assistance in facilitating bi-electronic or sequential mono-electronic transfer, in the presence of a suitable bridging ligand.

Experimental

Synthesis of ligands and complexes

L^4

To 0.9 mmol diformylpyridine in 150 cm^3 MeOH was added 0.6 mmol tren in 100 cm^3 MeOH dropwise and the solution was stirred $\approx$1 h at 50–60 °C. After cooling and filtering 30 cm^3 MeCN was added and the volume reduced to 50 cm^3. On slow evaporation, chunky white crystals of product formed in 56% yield.

$[Cu_2L^4]X_2 \cdot S$, $X=ClO_4^-$, $S=2CH_2Cl_2$ (1);
$X=BF_4^-$, $S=0$ (2)

0.3 g (0.5 mmol) L^4 was dissolved in 30 cm^3 deoxygenated CH_2Cl_2 and 0.32 g (1.02 mmol) $Cu(MeCN)_4X$ dissolved in the minimum of deoxygenated MeCN was added. A deep brown colour developed, and black crystals were obtained on standing in air. Yield 45–65%. (If these complexes are allowed to stand 1–2 days in MeCN solution and then recovered from solution, their IR spectrum has broadened considerably, and shows the presence of ν(CO) and ν(NH) absorptions, typical of hydrolysis.)

$[Cu_2L^4]X_3$, $X=BF_4$ (3)

0.3 mmol **1** in 5 cm^3 MeCN was treated with 0.30 mmol $FcBF_4$, and the solution evaporated quickly to dryness. The product was thoroughly washed with $CHCl_3$ to remove ferrocene. Yield $\approx$80%.

L^5

4 g L^4 was suspended in 400 cm^3 MeOH at reflux. $NaBH_4$ was added as solid in large excess until no further effervescence was noted. On removal of solvent,

the residue was dissolved in strong NaOH solution, which was then extracted with $CHCl_3$. The chloroform extract was washed with water, dried over Na_2SO_4, and reduced to a waxy solid, which was pumped several days to remove traces of solvent.

$[Cu_2L^5](ClO_4)_4 \cdot MeCN$ or $3H_2O$ (4 or 5)

0.3 g (0.5 mmol) L^5 was dissolved in 30 cm^3 1:1 EtOH/MeCN mixed solvent and 0.37 g (1 mmol) $Cu(ClO_4)_2 \cdot 6H_2O$ dissolved in 20 cm^3 EtOH was added. Blue powder, **5**, precipitated and was recrystallized from EtOH/MeCN to give bright blue crystals, **4**. Yield ≈77%.

$[Cu_2L^5(N_3)](ClO_4)_3$ (6)

0.3 g (0.5 mmol) L^5 was dissolved in 30 cm^3 EtOH/MeCN (1:1) and 0.37 g (1 mmol) $Cu(ClO_4)_2 \cdot 6H_2O$ was added, followed by 0.5 mmol NaN_3 dissolved in 5 drops of water. A colour change to green was noted, and on standing in air bright green crystals of product were obtained in ≈40% yield.

X-ray data

Crystal data. $[Cu_2L](ClO_4)_2 \cdot 2CH_2Cl_2$, $C_{35}H_{43}Cl_6Cu_2N_{11}O_8$, brown block, crystal dimensions 0.68×0.54×0.24 mm, monoclinic, $a = 27.256(8)$, $b = 10.970(3)$, $c = 18.941(6)$ Å, $\beta = 128.37(3)°$, $U = 4440(2)$ Å^3, $\mu = 1.38$ mm^{-1}, space group $C2/c$, $Z = 4$, $F(000) = 2216$.

Data were collected at −80 °C on a Nicolet R3m four-circle diffractometer using graphite-monochromated Mo Kα radiation ($\lambda = 0.71073$ Å). The unit cell parameters were determined by least-squares refinement of 25 accurately-centred reflections ($16 < 2\theta < 35°$) using 1.8° ω-scans at 4.88° min^{-1}; 4040 reflections were collected in the range $4 < 2\theta < 50°$. Of these, 3907 were unique and the 2783 having $F > 6\sigma(F)$ were used in the refinement. Crystal stability was monitored by recording three check reflections every 97 reflections and no significant variations were observed. The data were corrected for Lorentz and polarization effects and an empirical absorption correction was applied, based on ψ-scan data ($T_{min} = 0.721$, $T_{max} = 0.833$). The structure was solved by direct methods using the program TREF [19] which revealed the positions of all the non-hydrogen atoms. It was refined by full-matrix least-squares techniques. All the non-hydrogen atoms were assigned anisotropic thermal parameters. Hydrogen atoms were inserted at calculated positions, using a riding model with a common, fixed isotropic thermal parameter. The refinement, on 281 parameters, converged with $R = 0.051$ and $R_w = 0.061$. The function minimized in the refinement was $\Sigma w(F_o - F_c)^2$ where $w = [\sigma^2(F_o) + 0.0006F_o^2]^{-1}$. The final difference map showed no significant residual electron density. All programs used in data reduction, structure solution and refinement are contained in the SHELXTL-PC package [19]. Atomic coordinates are listed in Table 4.

TABLE 4. Atomic coordinates (×10^4)

	x	y	z
Cu	4626(1)	2235(1)	2848(1)
N(1)	4163(2)	2452(4)	3784(3)
C(1)	4057(3)	1178(5)	3869(3)
C(2)	4472(2)	326(4)	3802(3)
N(2)	4374(2)	556(3)	2969(3)
C(3)	4086(2)	−237(4)	2348(3)
C(4)	3889(2)	4(4)	1450(3)
C(5)	3448(2)	−762(4)	737(3)
C(6)	3202(2)	−454(5)	−124(3)
C(7)	3404(2)	609(5)	−261(3)
C(8)	3872(2)	1305(4)	492(3)
N(3)	4113(2)	1023(3)	1333(3)
C(9)	4121(2)	2343(5)	314(3)
N(4)	4663(2)	2799(4)	896(3)
C(10)	4875(2)	3695(5)	553(4)
C(11)	5305(2)	3060(5)	411(4)
C(12)	3607(2)	3185(5)	3142(3)
C(13)	3408(2)	3110(5)	2190(3)
N(5)	3945(2)	3501(4)	2236(3)
C(14)	3942(2)	4614(4)	2037(3)
C(15)	4492(2)	5250(4)	2240(3)
C(16)	4472(3)	6519(5)	2217(4)
C(17)	5000	7167(7)	2500
N(6)	5000	4608(5)	2500
Cl(1)	1834(1)	2110(1)	2418(1)
O(1)	1934(2)	2247(3)	3247(2)
O(2)	1942(2)	3259(4)	2179(3)
O(3)	2261(2)	1226(4)	2539(3)
O(4)	1201(2)	1733(5)	1731(3)
Cl(2)	1546(1)	1107(2)	5103(1)
C(20)	2156(3)	113(6)	5874(4)
Cl(3)	2210(1)	−1124(2)	5330(1)

Electrochemistry

Electrochemical measurements were made in MeCN solution using an EG&G PAR model 362 and a three-electrode cell with Pt or glassy carbon working electrode. Scan rates were in the range 10–100 mV s^{-1}.

ESR spectra were obtained with a Varian E109 spectrometer, ^{1}H NMR were obtained at QUB using 300 and 500 MHz spectrometers or by the SERC high-field 400 MHz NMR service at Warwick. Other physical measurements were obtained as described earlier [20].

Supplementary material

χ/T observations and fit to Bleaney Bowers equation are available from the authors on request.

Acknowledgements

We thank the Open University Research Committee and SERC for support (to D.M. and L.Q.) as well as for access to SERC services (high-field NMR at Warwick, and FAB-MS at Swansea). Thanks are also due to Mr Richard Murphy of QUB for assistance in obtaining the 500 MHz NMR spectra.

References

1 J.J.R. Frausto da Silva and R.J.P. Williams, *The Biological Chemistry of the Elements: the Inorganic Chemistry of Life*, Clarendon, Oxford, 1991.
2 D. McDowell and J. Nelson, *Tetrahedron Lett., 29* (1988) 385; J. Jazwinksi, J.-M. Lehn, D. Lilienbaum, R. Ziessel, J. Guilheim and C. Pascard, *J. Chem. Soc., Chem. Commun.,* (1987) 1691.
3 M.G.B. Drew, J. Hunter, D. Marrs and J. Nelson, *J. Chem. Soc., Dalton Trans.,* (1992) 11.
4 M.G.B. Drew, J. Hunter, D.J. Marrs, C.J. Harding and J. Nelson, *J. Chem. Soc., Dalton Trans.,* (1992) 3235.
5 C. Harding, V. McKee and J. Nelson, *J. Am. Chem. Soc.,* (1991) 9684.
6 M. McCann, L. Qin and J. Nelson, *Inorg. Biochem.,* in press.
7 D. Marrs, *Ph.D. Thesis,* Open University, Milton Keynes, 1990.
8 D. Marrs, N. Martin, V. McKee and J. Nelson, *Proc. Conf. Cu, Zn Triads, Edinburgh, UK, 1992.*
9 L. Qin, V. McKee and J. Nelson, in preparation.
10 V. McKee, D. Marrs and J. Nelson, *Polyhedron, 8* (1989) 1143.
11 V. McKee, D. Marrs, J. Nelson and W.T. Robinson, *Tetrahedron Lett.,* (1989) 7453.
12 M.G.B. Drew, G. Morgan, D. Marrs and J. Nelson, in preparation.
13 K.D. Karlin and Y. Gultneh, *Prog. Inorg. Chem., 35* (1985) 219.
14 S.M. Nelson, A. Lavery, J.-T. Grimshaw, K.P. McKillop and M.G.B. Drew, in K.D. Karlin and J. Zubieta (eds.), *Biological and Inorganic Copper Chemistry,* Adenine, New York, 1984, p. 27.
15 Q. Lu, J. Nelson, C. Harding and V. McKee, *Inorg. Biochem., 47* (1992) 51 and 55.
16 N.D. Chasteen and R.L. Belford, *Inorg. Chem., 9* (1970) 169.
17 J.E. Pate, T.J. Thamann and E.I. Solomon, *Spectrochim. Acta, Part A, 42* (1986) 313; J.E. Pate, P.K. Ross, T.J. Thamann, C.A. Reed, K.D. Karlin, T.N. Sorrell and E.I. Solomon, *J. Am. Chem. Soc., 111* (1989) 5198.
18 M.G.B. Drew, M. McCann and S.M. Nelson, *J. Chem. Soc., Dalton Trans.,* (1981) 1868; *Inorg. Chim. Acta, 1* (1980) 41.
19 G.M. Sheldrick, *SHELXTL-PC* (Version 4.1), Siemens Analytical X-ray Instruments Inc., Madison, WI, 1989.
20 C. Harding, D. McDowell, J. Nelson, S. Raghunathan, C. Stevenson, M.G.B. Drew and P. Yates, *J. Chem. Soc., Dalton Trans.,* (1990) 2521.